Journal of Power Sources 185 (2008) 542–548

Contents lists available at ScienceDirect

Journal of Power Sources

journal homepage: www.elsevier.com/locate/jpowsour

High reversible capacities of graphite and SiO/graphite with solvent-free solid polymer electrolyte for lithium-ion batteries

Y. Kobayashi [a,*], S. Seki [a], Y. Mita [a], Y. Ohno [a], H. Miyashiro [a], P. Charest [b], A. Guerfi [b], K. Zaghib [b]

[a] Central Research Institute of Electric Power Industry, 2-11-1 Iwado-kita, Komae, Tokyo 201-8511, Japan
[b] Institut de recherche, Hydro Québec, 1800, boul. Lionel-Boulet, Varennes, QC J3X 1S1, Canada

ARTICLE INFO

Article history:
Received 25 March 2008
Received in revised form 19 May 2008
Accepted 19 May 2008
Available online 3 June 2008

Keywords:
Lithium-ion polymer battery
Solid polymer electrolyte
Graphite
Silicon monoxide
Lithium iron phosphate
Overcoating

ABSTRACT

The combination of graphite or silicon monoxide (SiO)/graphite = 1/1 mixture with a solvent-free solid polymer electrolyte (SPE) was fabricated using a new preparation process, involving precoating the electrode with vapor-grown carbon fiber (VGCF) and binders (polyvinyl difluoride: PVdF or polyimide: PI), followed by the overcoating of the SPE. The reversible capacity of [graphite | SPE | Li] and [SiO/graphite | SPE | Li] cells were >360 and >1000 mAh g^{-1} with 78% and 77% for the 1st Coulombic efficiency, respectively. The reversible capacities were 75% at the 250th cycle for [graphite | SPE | Li] and 72% at the 100th cycle for [SiO/graphite | SPE | Li]. The electrode used was compatible with that of the conventional liquid electrolyte system, and the SPE film could be formed on the electrode by the continuous overcoating process, which will lead to a low-cost electrodes and low-cost battery production. The solid-state lithium-ion polymer battery (SSLiPB) developed in this study, which consisted of [$LiFePO_4$ | SPE | graphite], showed the reversible capacity of 128 mAh g^{-1} (based on the $LiFePO_4$ capacity) with favorable cycle performance.

1. Introduction

Lithium-ion batteries are now the main energy storage source for mobile electric devices. The energy density of the present cylindrical cell (18650) is approximately twice that of the 1st generation cells. Therefore, a suitable strict safety management is now more critical. In addition, other energy storage markets are emerging, such as a large battery energy system (BES) with wind power generation (WPG). Such large BES systems require more safety and also lower cost than the batteries for mobile use. To address some of these concerns, we have focused on the solid polymer electrolyte (SPE) and low-cost electrode materials, for example, lithium iron phosphate ($LiFePO_4$) [1], graphite, and silicon monoxide (SiO) [2]. Among them, $LiFePO_4$ showed good cycle performance at the high temperature of 60 °C [3]. We also recently reported stable battery performance with the [$LiFePO_4$ | SPE | Li] cell [4]. On the other hand, the anode material previously used with SPE was lithium metal or lithium titanate ($Li_4Ti_5O_{12}$) [5] because graphite or SiO were believed to be difficult to form a stable solid electrolyte interface (SEI) between graphite or SiO with SPE during intercalation [6]. Lithium metal is suitable for high-energy density batteries because of its high capacity, but the production line requires a sensitive moisture-controlled system, thus the production cost may be higher than that of the conventional lithium-ion battery. $Li_4Ti_5O_{12}$ is capable of achieving long-term cycle reversibility, its relatively higher potential (1.55 V vs Li/Li^+) is the main disadvantage when considering energy density. Recently, improvements in the reversibility of graphite [7] as well as SiO-related materials with SPE [8] were reported. Imanishi et al. reported the improved reversibility by surface modification of graphite [7]. It was a notable approach to actively control the SEI from the graphite surface. The surface modification did improve performance some degree, but we recognized that further effort is needed to obtain more improvement. Liu et al. reported results for the combination of SiO/$Li_{2.6}Co_{0.4}N$ composite and SPE [8]. Their results showed improvement in reversibility, but cobalt-related materials are not suitable for our low-cost target. In their preparation method, Liu et al. did not use any conductive additive in the electrode. In previous reports with the combination of graphite with SPE, acetylene black (AB) was generally used as a conductive additive. The surface area of AB depends on the manufacturer, varying between 50 and 100 m^2 g^{-1}. Note that electronic conductive additives such as AB may also act as active materials in the anode. The carbon materials with large surface area exhibit large irreversible capacity in cells with SPE [9] suggesting that we should select negative materials (electrode and also electronic conductive additives) with lower surface area. Vapor-grown carbon fiber (VGCF) is known to be a high-performance conductive additive with low surface area

* Corresponding author. Tel.: +81 3 3480 2111; fax: +81 3 3480 3401.
E-mail address: kobayo@criepi.denken.or.jp (Y. Kobayashi).

0378-7753/$ – see front matter © 2008 Elsevier B.V. All rights reserved.
doi:10.1016/j.jpowsour.2008.05.067

(<15 $m^2 g^{-1}$). Here, we applied VGCF as the conductive additive to minimize the total electrode surface area with sufficient electric conductivity. We also focused on the binder materials for anodes. In general, electrodes for solid polymer batteries consisted of active material, conductive additives and SPE [10]. Among them, SPE has also been used as ionic conductive additive as well as a binder. However, the binding property of the polyether-based structure is not very high. In particular, a stronger binding property is required in the case of silicon-based anodes because of their large volume change. Here, we introduce polyvinylidene difluoride (PVdF) binder for graphite and polyimide (PI) binder for SiO/graphite in the anode to maintain good electric contact between particles. This procedure was used for normal electrode preparation in conventional lithium-ion batteries. In our research, we introduce SPE onto the electrode using an overcoating technique. The overcoating procedure is described in the experimental section. In this paper, we report the combination of a graphite or SiO/graphite anode with SPE using VGCF and suitable binders. We also demonstrate a solid-state lithium-ion polymer battery (SSLiPB) with a [$LiFePO_4$ | SPE | graphite] cell.

2. Experimental

2.1. Electrode preparation

The anode materials were spherical natural graphite (Hydro Québec (HQ), average particle size: 12 μm; BET surface area: 4 $m^2 g^{-1}$) and SiO (average particle size: 8 μm; BET surface area: 8 $m^2 g^{-1}$). SiO was coated with carbon by a chemical process to enhance its electric conductivity. The detailed information will be reported elsewhere [11]. The graphite anode was a mixture of graphite (93 wt.%), VGCF (Showa Denko, 2 wt.%), and PVdF (Kureha, 5 wt.%). The SiO/graphite anode was a mixture of SiO (41.5 wt.%), graphite (41.5 wt.%), VGCF (2 wt.%), and PI (Ube, 15%). The cathode material used was carbon-coated $LiFePO_4$ (Phostech Lithium, average particle size: 50–250 nm; BET surface area: 13 $m^2 g^{-1}$). The $LiFePO_4$ cathode consisted of a mixture of $LiFePO_4$ (83 wt.%), VGCF (3 wt.%), Ketjenblack (3 wt.%), and PVdF (11 wt.%). The solvent used for the slurry was *N*-methyl pyrrolidone (NMP). The electrode slurries were coated on Cu foil (anode) or Al foil (cathode) using a coating machine (HQ).

2.2. Polymer overcoating

We used two kinds of SPE for overcoating. One (SPE1) was a high-molecular-weight (m.w. >1,000,000) ether-based polymer (P(EO/MEEGE) = 88/12, DAISO) [10]; EO is ethylene oxide, and MEEGE is 2-(2-methoxyethoxy) ethyl glycidyl ether. Lithium bis(trifluoromethylsulfonyl) imide (LiTFSI, 3 M) was added in the molar ratio [O]/[Li] = 16/1. P(EO/MEEGE) and LiTFSI were dissolved in acetonitrile (AN). The weight ratio of [P(EO/MEEGE) + LiTFSI]/[AN] was 1/9. Then, the SPE/AN solution was dripped onto the electrode using a micropipette to impregnate the solution into the electrode. After drying to remove AN, another cross-linked polymer sheet (P(EO/MEEGE/AGE) = 82/18/2, DAISO); where AGE is allyl glycidyl ether was placed on the overcoated electrode to enhance the mechanical properties of SPE. This procedure is suitable for small-sized electrodes such as those used in coin-type cells. The above procedure was conducted in a helium-filled glove box (VAC) at HQ.

Another SPE (SPE2) was made from ether-based low-molecular-weight cross-linkable polymer precursor (TA210, Daiichi Kogyo Seiyaku) [12]. LiTFSI was added at the ratio of [O]/[Li] = 30/1 in the precursor. After adding 1000 ppm of a UV cross-link initiator, the precursor was coated onto the electrode using the coating machine. Because the coating machine is equipped with an UV lamp, the precursor was cross-linked immediately on line. Additional SPE was not necessary because the overcoated polymer was well cross-linked, and it exhibited sufficient mechanical properties. The procedure was suitable for large electrodes, and very well adapted for large-scale productions. The above mentioned on-line coating procedure was conducted in a dry room at HQ. The thickness of overcoated SPE layer was approximately 50–70 μm. The ionic conductivities of SPEs in this study were about 10^{-3} S cm^{-1} at 60 °C.

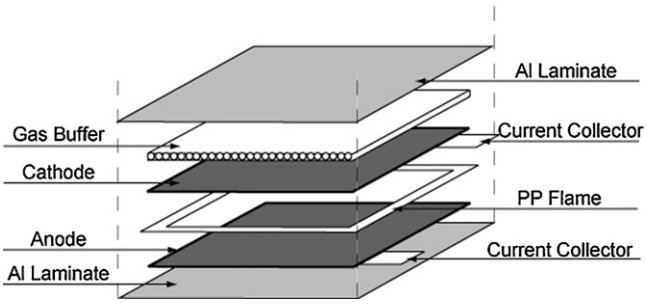

Fig. 1. Schematic representation of flat-type cell.

2.3. Cell preparation

All electrodes were dried overnight at 80 °C in vacuum prior to use. The electrochemical properties were mainly determined using a 2032 coin-type cell. The working and counter electrode (lithium metal, FMC, 0.2 mm thickness) areas were 2 cm^2 (Ø 16 mm). We also used a conventional organic electrolyte as a reference with a porous separator (Celgard). Its composition was 1 mol kg^{-1} lithium hexafluorophosphate ($LiPF_6$) in ethylene carbonate (EC)/dimethyl carbonate (DEC) with a 3/7 volume ratio (Ube). The coin-type cell was fabricated in the glove box.

We also prepared flat-type cells using an aluminum laminate film. To avoid an internal short circuit at the edge of the electrode, we used a polypropylene frame (thickness 25 μm), as shown in Fig. 1. The active surface area was defined as the surface area inside the frame. Some of the flat-type cells included a gas buffer sheet to evacuate the cell and to maintain constant low pressure inside the cell. The vacuum treatment is beneficial for larger cells because the larger electrodes can maintain constant pressure. The gas buffer can accept a small amount of degassing such as occurs during the SEI formation of the anode while still having low pressure inside. This system is suitable with electrolytes having minimal vapor pressure. The flat-type cell without vacuum treatment was kept under pressure from outside during operation. The flat-type cell with a gas buffer and vacuum treatment could be operated without any external pressure. The cell temperature was held at 60 °C. The cell performance was determined using a Macpile (Bio-Logic SAS) between 0 and 2.5 V (graphite and SiO/graphite half cell), or 2.0 and 3.8 V (lithium-ion cell). The initial formation cycle to determine the capacity was performed at C/24 rate. The cycling studies were conducted at C/8 or C/16 rate.

3. Results and discussion

3.1. Graphite properties

The initial charge and discharge voltage profiles of graphite electrodes in EC/DEC (a), SPE1 (b), and SPE2 (c) are shown in Fig. 2. These profiles were obtained using coin-type cells. The obtained capacities and corresponding Coulombic efficiencies are listed in Table 1.

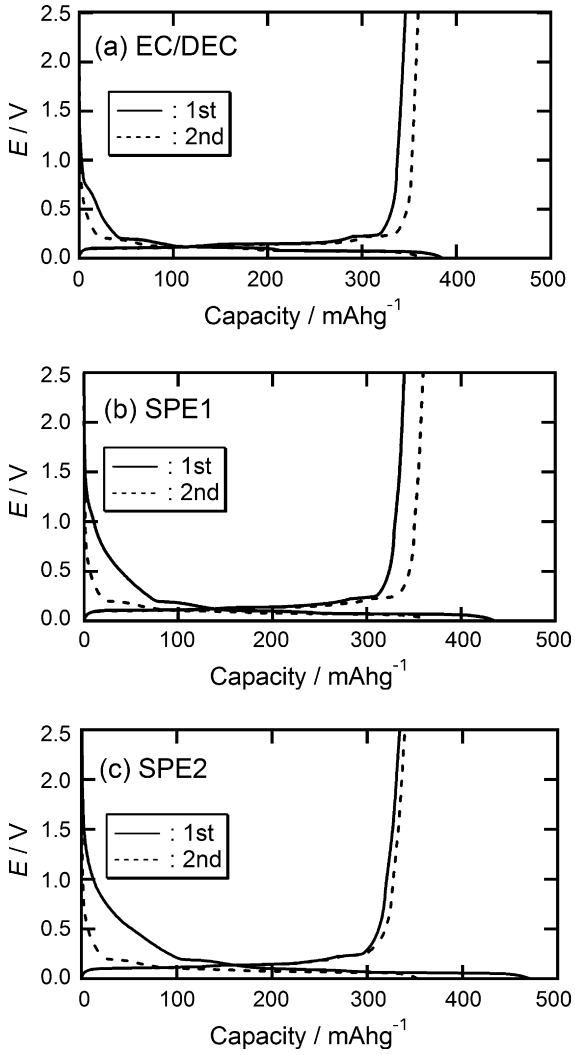

Fig. 2. Initial intercalation/deintercalation profiles of [graphite | electrolyte | Li] coin-type cell. Electrolytes are EC/DEC (a), SPE1 (b) and SPE2 (c). 2.5 V/0 V cutoff, C/24, 60 °C.

The reversible capacities of both SPEs were >330 mAh g^{-1}. For the 2nd cycle, the reversible capacity of SPE1 was 360 mAh g^{-1}, and it was compatible to that of the EC/DEC system. Coulombic efficiencies at the 1st cycle were 78% for SPE1 and 71% for SPE2. These values are still lower than that of the EC/DEC system (90%). However, the highest value previously reported was 65% in the graphite/SPE system, and it required the surface modification of the electrode by ball milling. Our results are higher values than that in the previous report, and they were obtained without any modification of the

Table 1
Intercalation/deintercalation capacities of graphite electrodes with various electrolyte systems

Electrolyte	1st capacity	2nd capacity	Ah efficiency	1st irrev. cap.
	Intercalation/deinterlacation [mAh g^{-1}]		1st/2nd [%]	[mAh g^{-1}]
EC/DEC/$LiPF_6$	386/346	362/360	90/99	40
SPE1[a]	436/340	365/360	78/99	94
SPE2[b]	472/334	353/340	71/96	134

[a] High-molecular-weight non-cross-linked SPE. Dripped on electrode with AN and dry. Then, add another cross-linked SPE.

[b] SPE on-line cross-linked on the electrode from cross-linkable precursor polymer.

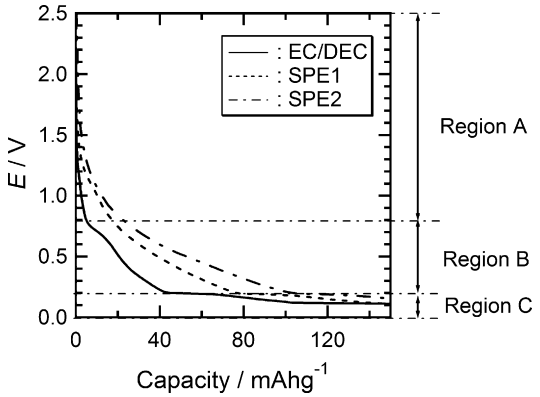

Fig. 3. The 1st intercalation voltage profiles of [graphite | electrolyte | Li] coin-type cell. Electrolytes are EC/DEC, SPE1, and SPE2.

electrode surface. Yazami and Deschamps had reported that the 1st Coulombic efficiency of their AB/SPE was 17% [9]. Although AB showed low Coulombic efficiency, they added 10 wt.% AB to other carbon active materials and used them as the electric conductive additives. As a result, the 1st Coulombic efficiencies of electrodes using other carbon materials were also low, between 30 and 60%. On the other hand, we used VGCF to decrease the weight ratio of the electric conductive additive. VGCF has good electronic conductive property with lower amount than other electronic conductive additives because of its unique structure consisting of long fibers. Furthermore, VGCF is prepared >2000 °C, consequently its surface area is lower than that of AB. We believe the lower surface area is responsible for the decrease in the irreversible capacity loss of the anode.

However, our results still required further improvement to reduce the irreversible capacity. Fig. 3 shows an expanded view of the 1st intercalation voltage profiles in the three electrolyte systems. To estimate the irreversible reaction region, we compared the capacity in the following three regions: Region A [2.5–0.8 V], Region B [0.8–0.2 V], and Region C [0.2–0 V]. These voltage regions were defined on the basis of the voltage profile of graphite with the EC/DEC system. We can see obvious inflection points at 0.8 and 0.2 V, and the voltage profile between these voltages were not evident for the following second intercalation process. That is, Region B in the EC/DEC system is considered the so-called “irreversible region”. We calculated the intercalation capacities in each region, and the obtained differential capacity between the 1st and the 2nd intercalation. Fig. 4 shows the numerical values of the differential capacity (inside the bar charts, mAh g^{-1}) and the normalized irreversible capacity ratio (bar charts) in the three electrolyte systems. As expected, the irreversible reaction occurred mainly in Region B for the EC/DEC system. Note that the irreversible capacity in Region C was negligible for the EC/DEC system, which suggested that the intercalation reaction proceeded without any side reaction in Region C after the SEI formation in Region B. On the other hand, large irreversible capacities in Regions A and C were observed as well as in Region B for SPE systems. These results suggest that the irreversible reaction process was quite different in the EC/DEC and SPE systems. At present, we cannot easily clarify where the SEI formation region is in the SPE systems. However, we believe that the SEI formation occurs in a wider voltage region in the SPE systems than in the EC/DEC system. The SEI is believed to be formed by reaction of the electrolyte components. In the case of the liquid electrolyte, an adequate ionic conductive path in the electrolyte is present even when some electrolyte decomposes at the electrode surface, because the liquid electrolyte has low viscosity. On the other hand, in the case of the SPE systems, the ionic conductive path may not be very good

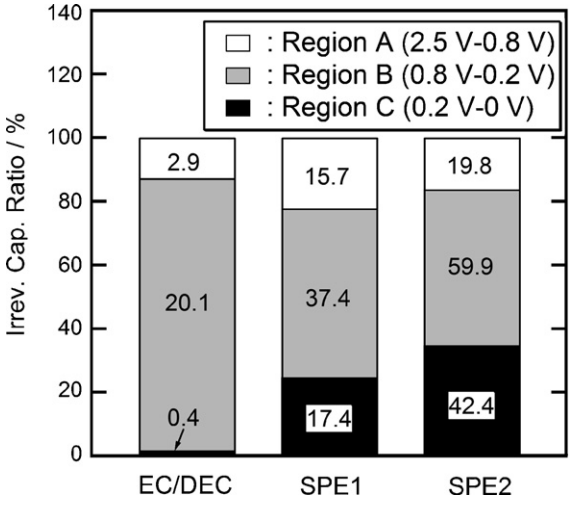

Fig. 4. Irreversible capacity ratio of graphite in each voltage regions using EC/DEC, SPE1, and SPE2. The values inside the bar chart are measured capacities (dimension: $mAh\,g^{-1}$).

because of the high viscosity of SPE, which may lead to larger irreversible capacity. In other words, SPE with high viscosity might not attach perfectly with the electrode during the 1st intercalation. Alternatively, the initial irreversible capacity may be related to the chemical stability of the electrolyte and the thickness of the SEI. The difference in the irreversible capacity between SPE1 and SPE2 may also support the above assumptions. As mentioned in the experimental section, the surface at the electrode comprised a non-cross-linked (in other words, "soft") polymer, so we added another cross-linked polymer onto it to prevent an internal short circuit. On the other hand, SPE2 was cross-linked on the electrode sheet, which indicates a relatively "hard" polymer. Therefore, we expect the natural trend is that the hard polymer (SPE2) has more restricted flexibility. This should lead to higher irreversible capacity during SEI formation than that obtained with the soft polymer. Although further optimization is needed to reduce the irreversible capacity, our results are encouraging, showing that graphite and SPE can yield high reversible capacity.

Fig. 5 shows the cycle performance of the [graphite | SPE1 | Li] coin-type cell at a rate of C/8. The initial deintercalation capacity was 350 $mAh\,g^{-1}$, and 75% reversible capacity was maintained at the 250th cycle. Coulombic efficiency was almost 100% in these cycles, which indicates that the combination of graphite with SPE is stable during long-term cycles. We believe that the electrodes produced using PVdF binder adequate electric contact between the electroactive particles and are able to accommodate volume changes that occur during long-term cycling.

3.2. SiO/graphite properties

The initial charge and discharge profiles of SiO/graphite electrodes with EC/DEC (a) and SPE1 (b) in coin-type cells at C/24 are shown in Fig. 6. The obtained capacities and corresponding Coulombic efficiencies are listed in Table 2. SPE1 showed high reversible capacities of over 1000 $mAh\,g^{-1}$ comparable to that obtained with the EC/DEC system. These reversible capacities are approximately twice larger than that from a previous report [8].

Coulombic efficiencies for the 1st cycle are 77% for SPE1 and 79% for EC/DEC. In contrast with the graphite electrode mentioned

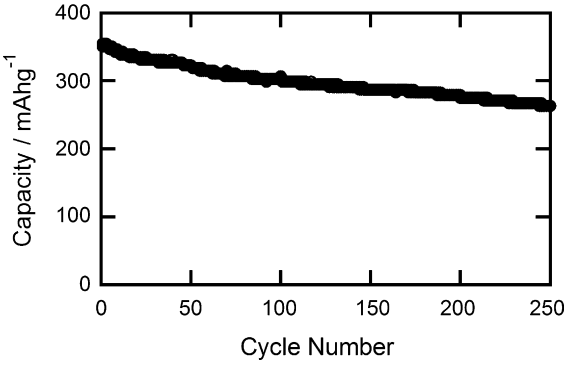

Fig. 5. Cycle performance of [graphite | SPE1 | Li] coin-type cell. 2.5 V/0 V cutoff, C/8, 60 °C.

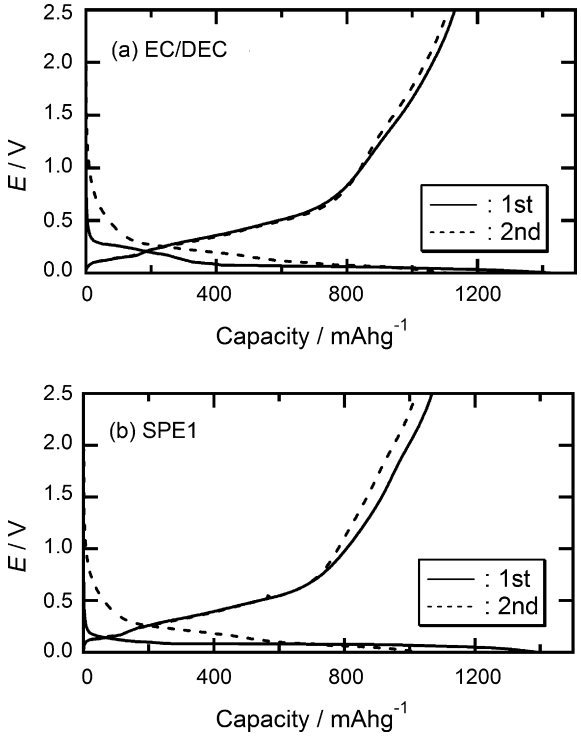

Fig. 6. Initial intercalation/deintercalation profiles of [SiO/graphite | electrolyte | Li] coin-type cell. Electrolytes are EC/DEC (a) and SPE1 (b). 2.5 V/0 V cutoff, C/24, 60 °C.

Table 2
Intercalation/deinterlation capacities of SiO/graphite electrodes with various electrolyte systems

Electrolyte	1st capacity	2nd capacity	Ah efficiency	1st irrev. cap.
	Intercalation/deinterlacation [$mAh\,g^{-1}$]		1st/2nd [%]	[$mAh\,g^{-1}$] (graphite/SiO)
$EC/DEC/LiPF_6$	1438/1131	1112/1109	79/100	307 (20[a]/287[b])
SPE1	1394/1068	1031/1020	77/99	326 (47[a]/289[b])

[a] Calculated irreversible capacity derived from graphite. The irreversible capacity of graphite referred to Table 1.
[b] Calculated irreversible capacity derived from SiO, which was calculated by the subtracting the graphite contribution from the total irreversible capacity.

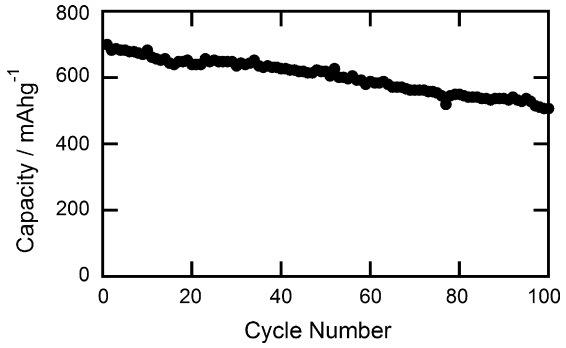

Fig. 7. Cycle performance of [SiO/graphite | SPE1 | Li] coin-type cell. 2.5 V/0 V cutoff, C/8, 60 °C.

in Table 1, the Coulombic efficiency of SPE was about 10% lower than that of EC/DEC. This small difference in Coulombic efficiency of only 2% between SPE1 and EC/DEC with the SiO/graphite is explained as follows. It is clear that the main contribution to the irreversible capacity is attributed to the electrochemical properties of SiO because the irreversible capacity is similar in the two electrolyte systems. This suggests that the irreversible reaction of SiO has a weak correlation with electrolyte species. The origin of the irreversibility in Si-related materials had been reported to be mainly derived from the irreversible reaction inside the particle, such as a large volume change during deep intercalation [13]. Therefore, as the relative contribution of SEI formation involving reaction of the electrolyte in the irreversible reaction was smaller with the SiO/graphite than in graphite, Coulombic efficiency is dominated by irreversible contribution from the reactivity of SiO. The net effect is that the SiO/graphite has similar Coulombic efficiencies in EC/DEC and SPE1.

Fig. 7 shows the cycle performance of the [SiO/graphite | SPE1 | Li] coin-type cell at C/8 rate. The initial deintercalation capacity was 700 mAh g^{-1}, and 72% reversible capacity was maintained at the 100th cycle. These results for the reversible capacity and cycle life stability are higher than those from a previous report [8]. The initial reversible capacity decreased to 70% versus that in C/24 operation (1020 mAh g^{-1}) because the cell voltage reached 0 V earlier in C/8 than in C/24. This suggested that the interfacial impedance with SiO/graphite | SPE1 was higher than that with graphite | SPE1 at around 0 V (fully intercalated state). We assumed that SPE1 could not accommodate the large volume change of SiO/graphite in the deep intercalation state at the C/8 rate. We also applied the combination of SPE2 and SiO/graphite, but the obtained reversible capacity was poor (<40 mAh g^{-1}) even at C/24 rate. This suggests that the hard polymer cannot accommodate the large volume change of SiO/graphite particles that occurs during charge/discharge cycling. The introduction of a more flexible polymer may be one way of improving the cycle life in the SiO/graphite system. Even though further improvement in reversibility is still required, SiO/graphite has the potential to be a higher capacity anode than graphite in the SPE system.

3.3. Flat-type cell properties

As mentioned in the experimental section, SPE2 was overcoated onto the electrodes without additional SPE or a porous separator, which is one of a high-cost material in a battery. Furthermore, there is no need for a filling step and immersion process that are required with a conventional liquid electrolyte system. We can prepare an all solid-state battery just gluing together a cathode and an anode. The basic concept of the cell preparation process using overcoated electrodes is shown in Fig. 8. The anode and cathode are fabricated using a conventional process that is used with electrodes for liquid electrolyte system. These electrodes are further processed to form a cell sheet (see Fig. 8) by overcoating SPE, cross-link, and glued together in a continuous on-line process. We believe this process will be cheaper than the conventional preparation system using liquid electrolyte because all steps can occur continuously on one line.

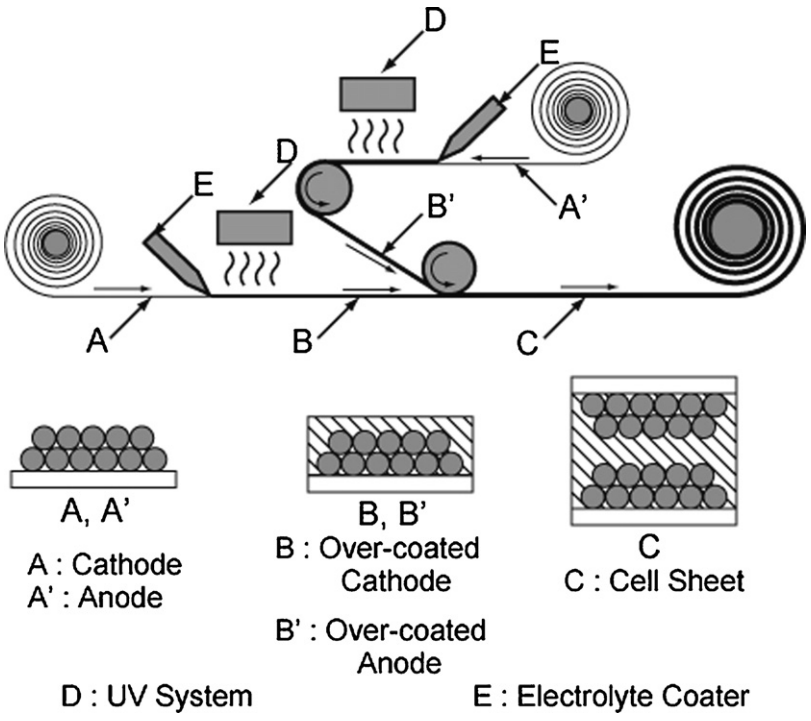

Fig. 8. The basic concept of the cell preparation process using overcoated electrodes.

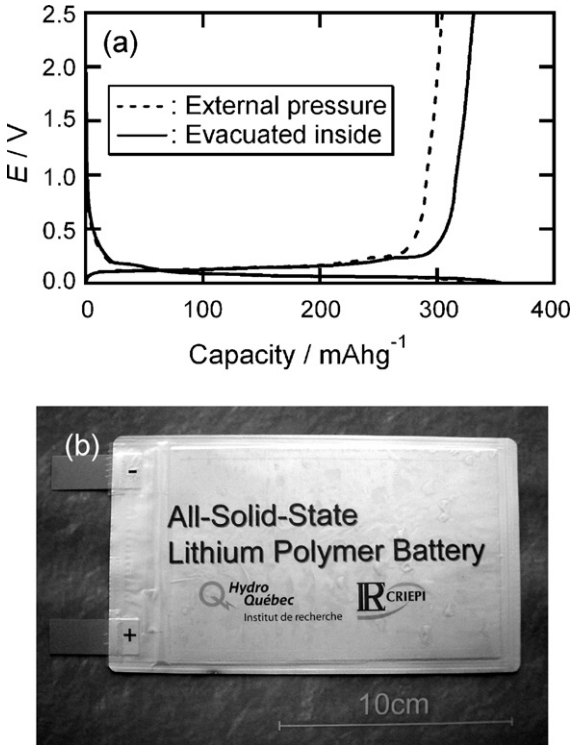

Fig. 9. Voltage profiles of flat-type cells (13 cm × 8 cm) at 2nd cycle. (a) [graphite | SPE2 | Li] cell. 2.5 V/0 V cutoff, C/24, 60 °C. Dashed line: external pressure, solid line: evacuated inside. (b) Photograph of flat-type cell. Active area: 13 cm × 8 cm = 104 cm^2.

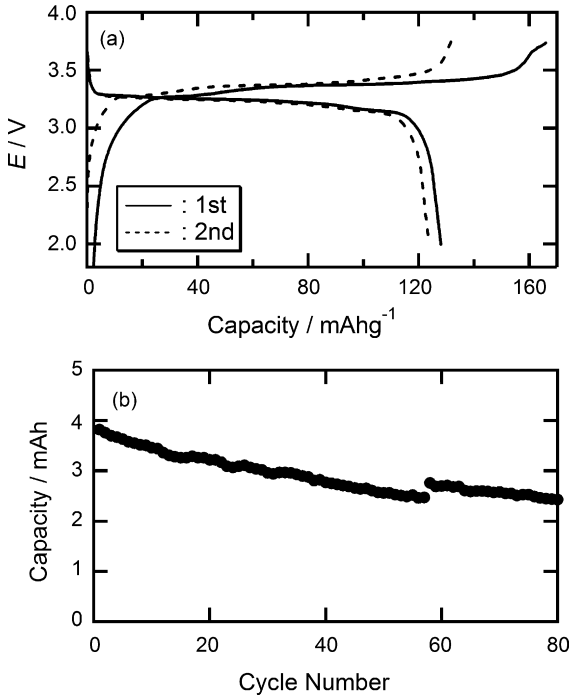

Fig. 10. Initial voltage profiles (a) and the following cycle performance (b) of solid-state lithium-ion polymer battery (SSLiPB). Cell size: 4.5 cm × 3.5 cm = 15.8 cm^2. 3.8 V/2.0 V cutoff, C/24 in initial 2 cycles, C/16 in cycle test, 60 °C.

To demonstrate scale-up of the process outlined in Fig. 8, we prepared flat-type cells using aluminum laminate. The active surface area is 104 cm^2 (13 cm × 8 cm), and the cells were compressed by external pressure or evacuated inside using gas buffer as shown in Fig. 1. Fig. 9 shows the 2nd charge and discharge profiles of [graphite | SPE2 | Li] (a) cells with external pressure (dashed line) and with vacuum (solid line). To maintain a vacuum, a gas buffer was used as shown in Fig. 1. A photograph of one of these cells is presented in Fig. 9(b). The reversible capacities were 305 mAh g^{-1} (external pressure) and 331 mAh g^{-1} (evacuated), suggesting that the evacuated process leads homogeneous contact in the higher area SPE. This feature permitted cell operation without the use of external pressure which is a very advantageous feature for large-cell production.

Finally, we undertook an effort to fabricate a "solid-state lithium-ion polymer battery" (SSLiPB). Although many types of so-called "lithium-ion polymer batteries" have been reported, an organic liquid electrolyte is a key component because of poor reversibility of graphite with SPE. Fig. 10 shows the initial charge and discharge voltage profiles (a) at C/24 rate and the cycling results (b) at C/16 rate obtained with a SSLiPB. In this example, SPE1 was selected because of its better reversibility at the 1st cycle, and we added another SPE between electrodes. The cell area is 15.8 cm^2 (3.5 cm × 4.5 cm), and the cell was evacuated. The initial discharge capacity was 128 mAh g^{-1} (based on the capacity of $LiFePO_4$), and the corresponding Coulombic efficiency was 77%. The irreversible capacity was mainly derived from the graphite (see in Table 1). The initial average voltage was 3.18 V at C/24 rate. The capacity retention at the 80th cycle was approximately 64% relative to the initial state at C/16. Even though further improvement in performance is required, the results obtained with this initial SSLiPB test are very encouraging, particularly because no solvent was used in the cell. Further effort will focus on improving the cycle properties by optimization of the overcoating process, the electrode balance, and the cell design.

4. Conclusion

The combination of graphite or SiO/graphite with SPE was evaluated using an innovative process, involving precoating of the electrode with VGCF and binder, followed by the overcoating of SPE. The reversible capacities were 360 mAh g^{-1} for graphite and >1000 mAh g^{-2} for SiO/graphite. The reversible capacity was 75% at the 250th cycle versus the initial capacity for graphite, and 72% at the 100th cycle for SiO/graphite. The irreversible reaction of graphite with SPE was different from that of graphite with EC/DEC. These results are attributed to the difference in the reactivity of the electrolyte with graphite (formation of SEI). On the other hand, the irreversible capacities of SiO/graphite in the liquid electrolyte and SPE were similar because the reaction responsible for the irreversible capacity was not due to the SEI formation but instead from the volume change of the particles during cycling.

Initial results with flat-type half-cell and flat-type SSLiPB using solvent-free SPE were demonstrated. The initial reversible capacity of the SSLiPB was 128 mAh g^{-1}, and the average voltage was 3.18 V. The component setup of the prepared SSLiPB has a potential to be a low-cost battery because; (i) the electrodes are fabricated by a process that shares technology used to conventional liquid electrolyte cells that are already optimized in cell production, (ii) a high-cost separator is not necessary, (iii) no need for a liquid filling process, (iv) adaptable to continuous one-line preparation using the overcoating process of SPE, and (v) the manufacturing steps can use similar conditions as with lithium-ion cells with liquid electrolyte. We should also add the improvement of safety because of the use of flammable solvent is not necessary, which is the most important issue for large battery systems. We believe that the SSLiPB has the potential to be used in large energy storage systems in the near future.

References

[1] A.K. Padhi, K.S. Nanjundaswamy, J.B. Goodenough, J. Electrochem. Soc. 144 (1997) 1188.
[2] T. Morita, N. Takami, J. Electrochem. Soc. 153 (2006) A425.
[3] K. Zaghib, N. Ravet, M. Gauthier, F. Gendron, A. Mauger, J.B. Goodenough, C.M. Julien, J. Power Sources 163 (2006) 1047.
[4] Y. Kobayashi, Y. Mita, S. Seki, Y. Ohno, H. Miyashiro, N. Terada, J. Electrochem. Soc. 154 (2007) A677.
[5] K. Zaghib, M. Simoneau, M. Armand, M. Gauthier, J. Power Sources 81–82 (1999) 300.
[6] F. Coowar, D. Billaud, J. Ghanbaja, P. Baudry, J. Power Sources 62 (1996) 179.
[7] N. Imanishi, Y. Ono, K. Hanai, R. Uchiyama, Y. Liu, A. Hirano, Y. Takeda, O. Yamamoto, J. Power Sources 178 (2008) 744–750.
[8] Y. Liu, J. Yang, N. Imanishi, A. Hirano, Y. Takeda, O. Yamamoto, J. Power Sources 146 (2005) 376.
[9] R. Yazami, M. Deschamps, J. Power Sources 54 (1995) 411.
[10] S. Matsui, T. Muranaga, H. Higobashi, S. Inoue, T. Sakai, J. Power Sources 97–98 (2001) 772.
[11] Y. Kobayashi, in preparation.
[12] M. Kono, M. Nishiura, E. Ishiko, J. Power Sources 81–82 (1999) 748.
[13] L.Y. Beaulieu, K.W. Eberman, R.L. Turner, L.J. Krause, J.R. Dahn, Electrochem. Solid-State Lett. 4 (2001) 137.